Physical–Chemical Behavior of Dietary and Biliary Lipids during Intestinal Digestion and Absorption. 1. Phase Behavior and Aggregation States of Model Lipid Systems Patterned after Aqueous Duodenal Contents of Healthy Adult Human Beings†

Joan E. Staggers,‡ Olle Hernell,§ Richard J. Stafford,∥ and Martin C. Carey*
Department of Medicine and Harvard Digestive Disease Center, Harvard Medical School, Gastroenterology Division, Brigham and Women's Hospital, Boston, Massachusetts 02115

Received March 6, 1989; Revised Manuscript Received September 19, 1989

ABSTRACT: We developed equilibrium phase diagrams corresponding to aqueous lipid compositions of upper small intestinal contents during lipid digestion and absorption in adult human beings. Ternary lipid systems were composed of a physiological mixture of bile salts (BS),[1] mixed intestinal lipids (MIL), principally partially ionized fatty (oleic) acid (FA) plus racemic monooleylglycerol (MG), and cholesterol (Ch), all at fixed aqueous-electrolyte concentrations, pH, temperature, and pressure. The condensed phase diagram for typical physiological conditions (1 g/dL total lipids, FA:MG molar ratio of 5:1, pH 6.5, 0.15 M Na^+ at 37 °C) was similar to that of a dilute model bile [BS/lecithin (PL)/Ch] system [Carey, M. C., & Small, D. M. (1978) *J. Clin. Invest. 61*, 998–1026]. We identified two one-phase zones composed of mixed micelles and lamellar liquid crystals, respectively, and two two-phase zones, one composed of Ch monohydrate crystals and Ch-saturated micelles and the other of physiologic relevance composed of Ch- and MIL-saturated mixed micelles and unilamellar vesicles. A single large three-phase zone in the system was composed of Ch-saturated micelles, Ch monohydrate crystals, and liquid crystals. Micellar phase boundaries for otherwise typical physiological conditions were expanded by increases in total lipid concentration (0.25–5 g/dL), pH (5.5–7.5), and FA:MG molar ratio (5–20:1), resulting in a reduction of the size of the physiological two-phase zone. Mean particle hydrodynamic radii ($\bar{R}_h$), measured by quasielastic light scattering (QLS), demonstrated an abrupt increase from micellar (<40 Å) to micelle plus vesicle sizes (400–700 Å) as this two-phase zone was entered. With relative lipid compositions within this zone, unilamellar vesicles formed spontaneously following coprecipitation, and their sizes changed markedly as functions of time, reaching equilibrium values only after 4 days. Further, vesicle $\bar{R}_h$ values were influenced appreciably by MIL:mixed bile salt (MBS) ratio, pH, total lipid concentration, and FA:MG ratio, but not by Ch content. In comparison, micellar systems equilibrated rapidly, and their $\bar{R}_h$ values were only slightly influenced by physical–chemical variables of physiological importance. In contrast to the BS–PL–Ch system [Mazer, N. A., & Carey, M. C. (1983) *Biochemistry 22*, 426–442], no divergence in micellar sizes occurred as the micellar phase boundary was approached. The ionization state of FA at simulated "intestinal" pH values (5.5–7.5) in the micellar and physiologic two-phase zones was principally that of 1:1 sodium hydrogen dioleate, an insoluble swelling "acid soap" compound. By phase separation and analysis, tie-lines for the constituent phases in the two-phase zone demonstrated that the mixed micelles were saturated with MIL and Ch and the coexisting vesicles were saturated with MBS, but not with Ch. These observations provide a fundamental framework for understanding the physical–chemical state of aqueous upper intestinal contents during lipid digestion and absorption in adult human beings [see Hernell et al. (1990) (companion paper)].[2]

Intestinal digestion and absorption of long-chain TG, the principal dietary lipid, involve several complex steps. These include emulsification, lipase hydrolysis of FA[1] ester linkages, aqueous dispersion of lipolytic products, and their absorption by upper small intestinal enterocytes (Borgström, 1977; Patton, 1981; Carey et al., 1983). The chemical compositions of lipids in upper intestinal contents following a lipid-rich meal in humans have been extensively defined [e.g., Hofmann and Borgström (1962, 1964), Porter and Saunders (1971), Thompson et al. (1971), Miettinen and Siurala (1971), and Mansbach et al. (1975)]. However, the physical–chemical nature and equilibria of the dispersed hydrolytic products are still incompletely understood (Carey et al., 1983).

† Supported in part by Research Grant DK 36588 and Center Grant DK 34854 (M.C.C.), NRSA Fellowship AM 07512 and Institutional Training Grant AM 07121 (J.E.S.), Fogarty International Fellowship TW 03521 (O.H.), and Research Training Grant AM 07333 (R.J.S.), all from the National Institutes of Health, U.S. Public Health Service. O.H. received grants-in-aid from the Swedish Medical Research Council, the Sweden–America Foundation, the Henning and Johan Throne Holst Foundation, and Pfrimmer/Meda AB (Sweden).

* Correspondence should be addressed to this author at the Department of Medicine, Brigham and Women's Hospital, 75 Francis Street, Boston, MA 02115.

‡ Present address: Merck, Sharp and Dohme Research Laboratories, Blue Bell, PA 19422.

§ Present address: Department of Pediatrics, University of Umeå, S-90185 Umeå, Sweden.

∥ Present address: Digestive Disease Associates P.A., 2545 Chicago Avenus S., Minneapolis, MN 55404.

[1] Abbreviations: BS, bile salt; MBS, mixed bile salts; MIL, mixed intestinal lipids (lipids dispersed in aqueous-rich portion of duodenal contents); Ch, cholesterol monohydrate; FA, fatty acid, oleic acid; TG, triacylglycerol, triolein; DG, diacylglycerol, diolein; MG, monoacylglycerol, monoolein; PL, phospholipid, diacylphosphatidylcholine; $\bar{R}_h$, mean hydrodynamic radius; R_h, hydrodynamic radius; QLS, quasielastic light scattering; cmc, critical micellar concentration; imc, intermicellar concentration.

[2] A preliminary report of this work has appeared (Staggers et al., 1986).

0006-2960/90/0429-2028$02.50/0

Hofmann and Borgström (1962, 1964) first reported that, during established fat digestion in human beings, luminal lipids, following ultracentrifugation, constituted two or three "phases": an upper oil phase, rich in TG and DG; a middle optically clear aqueous phase, presumed to be micellar; and a lower precipitate phase (pellet). On the basis of theoretical phase equilibria considerations (Carey, 1983), microscopy of TG hydrolysis products (Patton & Carey, 1979), and physical–chemical examination of aqueous intestinal contents from human volunteers, Stafford and colleagues (Stafford & Carey, 1981; Stafford et al., 1981) reported evidence for the existence of a dispersed liquid-crystalline phase in addition to emulsion particles and mixed micelles during lipid digestion and absorption in the upper small intestine (Carey et al., 1983; Borgström, 1985). However, precise information is lacking regarding the equilibria, sizes, and compositions of these dispersed lipid particles, as well as their origin, fate, and possible significance.

The present work describes a systematic phase equilibria investigation of model lipid systems, patterned according to the chemical compositions of aqueous lipids of the human upper small intestine during established fat digestion and absorption (Hofmann & Borgström, 1962; Ricour & Rey, 1970; Porter & Saunders, 1971; Thompson et al., 1971; Miettinen & Siurala, 1971; Mansbach et al., 1975). We have defined the complete condensed phase diagram of one system for typical physiological conditions. We have also determined the influence of several physical–chemical variables upon the phase boundaries and physical–chemical compositions of a two-phase zone, shown in the accompanying paper (Hernell et al., 1990) to be the most important pathophysiologically. In particular, we demonstrate that unilamellar vesicles of variable size and metastability form spontaneously within this zone and coexist with thermodynamically stable saturated mixed micelles with maximum hydrodynamic radii of ~40 Å.

Theoretical Considerations

Phase equilibria in accordance with the Gibbs phase rule were planned on the basis of the following criteria [reviewed in Carey (1983)]: (1) the aqueous lipid systems were at fixed temperature (37 °C) and pressure (1 atm), thereby eliminating two degrees of freedom; (2) the water concentration, one of the four components, was fixed ab initio, thereby reducing each system to a ternary one composed of three lipid "components". The lipid components were considered to behave as single chemical species, although two were lipid mixtures. This assumption was based on the following analogies: (1) a physiological BS mixture behaves as a single component at high dilution (95–99.5 g/dL H_2O) because the bile salts are members of a closely related family of molecules, forming MBS micelles above a critical micellar concentration (cmc) of ~0.1% (this work); (2) the MIL,[3] principally partially ionized FA ("acid soap") and MG, behave as a single component in dilute systems, since both are swelling amphiphiles (Small, 1971). Because it can be justified only a posteriori that a system containing 15 chemical species plus a buffered solvent behaves as a pseudo-three-component system (with tie-lines located within the triangle), we will show subsequently that these assumptions are reasonable, particularly under simulated physiological compositions and pH. By analogy with model biliary lipid systems (Carey, 1983), it follows that such a triangular phase diagram of MBS, MIL, and Ch will be defined by two one-phase zones, two two-phase zones, and one three-phase zone. Because temperature, pressure, and percent aqueous buffer were fixed from the outset, the Gibbs phase rule (Carey, 1983), as applied to this system, reduces to

$$F = C - P$$

where F represents the number of degrees of freedom, C the number of lipid components, and P the number of phases. Thus, at equilibrium, for mixtures of three lipid components that are soluble, swelling, and insoluble amphiphiles, respectively (Small, 1968), two compositions can be altered independently in each of the one-phase zones (either micellar or liquid crystalline) without a phase change occurring. In the two-phase zones, only one composition can be altered independently, and in the three-phase zone, the system is invariant.

Table I: Composition of Mixed Bile Salt (MBS) System[a]

species	mol wt	mol %
sodium glycocholate	487.6	24
sodium glycochenodeoxycholate	471.6	24
sodium glycodeoxycholate	471.6	16
sodium glycolithocholate	455.6	0.7
disodium glycolithocholate sulfate	557.6	3
sodium taurocholate	537.7	12
sodium taurochenodeoxycholate	521.7	12
sodium taurodeoxycholate	521.7	8
sodium taurolithocholate	505.7	0.3
disodium taurolithocholate sulfate	607.7	1
	av 502	

[a] This composition is the average of many published compositions [cf. Hofmann (1976)].

Experimental Procedures

Materials

Highest purity FA, racemic MG and DG, Ch (Nu-Chek Prep., Inc., Elysian, MN), and grade I egg phosphatidylcholine (lecithin, PL) (Lipid Products, Redhill, Surrey, England), were stored in sealed glass ampules at −20 °C prior to study. Conjugated BS (listed in Table I) were purchased from CalBiochem-Behring (San Diego, CA), purified as described (Carey & Small, 1978), and stored in a desiccator at 23 °C. By thin-layer chromatography (200-μg applications), all long-chain lipids and Ch were determined to be >99% pure as received. Following purification, individual BS species were generally >96% pure with respect to class. Since other BS conjugates (intended constituents of the MBS system) were occasional contaminants and no unconjugated (free) bile salts were detected, no further purification was attempted.

Solvents and other reagents were certified ACS grade obtained from Fisher Chemical Co. (Pittsburgh, PA). Purified 3α-hydroxysteroid dehydrogenase, for BS assays,[4] was purchased from Sigma Chemical Co. (St. Louis, MO). Reagent grade NaCl was roasted at 600 °C in a muffle furnace for 4 h to oxidize and remove organic impurities. Water was distilled in an all-glass Pyrex automatic still (Corning, NY), filtered to remove dust, boiled, and cooled under N_2 to remove

[3] To better approximate physiological lipid compositions (Miettinen & Siurula, 1971) 1–3 mol % DG, an insoluble nonswelling amphiphile (Small, 1971), was included in the MIL systems. Although such concentrations of DG substantially stabilize nonbilayer phases of PL systems (Siegel et al., 1989, and references cited therein), they did not appreciably influence the swelling amphiphile or bilayer properties of dilute aqueous intestinal lipid mixtures [see also Larsson (1967)].

[4] This enzyme is unreactive with 3α-sulfated BS, which constituted 4% of the MBS (Table I). Hence, all enzymatic estimates of BS concentrations were corrected upward appropriately.

Table II: Composition of Mixed Intestinal Lipid (MIL) Systems

composition	species	mol ratio	mol %	mol wt
A	oleic acid	5	69.4	283
	monoolein	1	13.9	357
	diolein	0.2	2.8	621
	lecithin	1	13.9	787
				av 372.8
B	oleic acid	10	82.0	283
	monoolein	1	8.2	357
	diolein	0.2	1.6	621
	lecithin	1	8.2	787
				av 335.8
C	oleic acid	20	90.0	283
	monoolein	1	4.5	357
	diolein	0.2	0.9	621
	lecithin	1	4.5	787
				av 312.1

dissolved atmospheric O_2 and CO_2.

Methods

Preparation of Lipid Mixtures. The BS mixture (MBS, Table I) was patterned after the average composition of human bile (Hofmann, 1976). MBS stock solutions were prepared gravimetrically and dissolved in spectroanalyzed CH_3OH, whereas stock solutions of all other lipids were prepared individually in $CHCl_3$; precise lipid concentrations were verified by dry weight determinations. Compositions of MIL solutions (listed in Table II) were prepared volumetrically from stock solutions to give molar ratios ranging from 5:1 to 20:1 in the principal lipids (FA and MG). Systems with intended compositions of all three components (MBS/MIL/Ch) were prepared by coprecipitation of lipid mixtures from $CHCl_3$/CH_3OH solutions, as previously described (Carey & Small, 1978). In brief, each MBS/MIL/Ch mixture was delivered, by volume, into 100 × 16 mm screw-capped tubes. Organic solvents were evaporated under a stream of N_2 and then under reduced pressure for 12–18 h to achieve constant weight. Unless otherwise specified, the aqueous buffer was 33 mM NaH_2PO_4/Na_2HPO_4 (pH 6.5) with 3 mM NaN_3 (to prevent microbial growth) and sufficient NaCl to give a final added Na^+ concentration of 150 mM. After the tubes were sealed with Teflon-lined screw caps under a blanket of N_2, they were vigorously vortex-mixed for a few minutes and then shaken continuously in a covered Dubinoff water bath at 37 °C. For determination of the condensed ternary phase diagram, approximately 400 mixtures were prepared and examined.

Examination of Lipid Mixtures. Aqueous lipid mixtures were examined in sealed tubes at hourly to daily intervals with the aid of a high-intensity light source, and their appearances (grades of cloudiness, turbidity or optical clarity) were recorded. Following equilibration at ~7 days (see Results), a few microliters of well-mixed samples was placed on a slide with cover slip and examined for the presence of crystals, liquid crystals, and oils by direct and polarizing light microscopy (Zeiss photomicroscope III, Carl Zeiss, Thornwood, NY). Mean hydrodynamic radii ($\bar{R}_h$) and variances (V), an index of particle polydispersity, were measured at 37 ± 0.5 °C by means of QLS (Mazer et al., 1976, 1979). In one set of experiments, $\bar{R}_h$ values were measured at frequent time intervals following sample preparation until equilibrium $\bar{R}_h$ values were achieved. Prior to QLS measurements, dust was sedimented by centrifugation of samples for 10 min–1 h at 10000 rpm in a model SS-4 Sorvall tabletop centrifuge (Newtown, CT). The theory and application of QLS to measurement of lipid particle sizes in analogous mixed lipid systems have been described (Mazer et al., 1979, 1980; Cohen et al., 1990). QLS instrumentation included a Spectra-Physics (Mountain View, CA) Model 164 argon ion laser (wavelength, 5145 Å) equipped with a Model 1096 Langley Ford autocorrelator (Amherst, MA) interfaced to a Digital Equipment Corp. (Marlboro, MA) Professional 350 computer with high data-storage capacity. For multicomponent particle analysis, autocorrelation functions were fitted to 1, 2, or 3 components by a splicing function as described (Cohen, 1986; Cohen et al., 1990). Particle number and lipid weight ratios in systems with two (or three) particle populations were calculated from their respective sizes (hydrodynamic radius, R_h) and fractions of scattered light, assuming a form factor of 1 for micellar particles and a form factor for unilamellar vesicles that was calculated on the basis of a lipid bilayer thickness of 40 Å (Cohen, 1986; Cohen et al., 1989).

To study dissolution kinetics of systems containing both saturated mixed micelles and unilamellar vesicles by unsaturated mixed micellar solutions, dust-free samples (described above) were combined in equal volumes of 300 μL in 6 × 50 mm glass tubes, mixed by rapid inversion, immediately placed in a sample holder at 37 ± 0.5 °C, and analyzed by QLS. $\bar{R}_h$ values were recorded at frequent time intervals until stable values were obtained.

Separation of Phases from Lipid Mixtures. Ch (monohydrate) crystals were pelleted by mild centrifugation conditions in a SS-4 Sorvall tabletop centrifuge (Newton, CT). Samples with liquid-crystalline and/or oil phases were separated into their constituent phases by tabletop ultracentrifugation (Beckman, Palo Alto, CA; Model TL-100) for 5 h at 100000g at 37 °C utilizing a TLS-55 swinging bucket rotor. Such separations consistently produced an isotropic mixed micellar subphase, as evaluated by QLS ($\bar{R}_h$ < 40 Å and V < 30%), without creating an appreciable BS concentration gradient throughout the centrifuge tubes (Porter & Saunders, 1971). However, in harvesting the floating nonmicellar phases, difficulties were frequently encountered in avoiding contamination by the micellar phase [see Mazer and Carey (1983)].

Chemical Analysis of Phases. Portions of original lipid mixtures, as well as all phases harvested following tabletop and ultracentrifugal separations, were first extracted from the aqueous system by a minor modification of the method of Folch and colleagues (Folch et al., 1957). To ensure full protonation and extraction of FA, the $CHCl_3$/MeOH phase was partitioned with 20% (v/v) 150 mM aqueous NaCl containing 2% glacial CH_3COOH (v/v) at pH ~3 (Staggers et al., 1982). The aqueous MeOH and $CHCl_3$ phases were then separated by centrifugation in a tabletop centrifuge at 2000 rpm for 10 min. Since, in preliminary experiments, BS partitioned into both upper (aqueous MeOH) and lower ($CHCl_3$) phases, both solvent phases were assayed for BS, using the enzymatic (3α-hydroxysteroid dehydrogenase) method (Turley & Dietschy, 1978) employing pure MBS solutions as standards. Since the $CHCl_3$ contained >95% of all long-chain lipids (and Ch), phospholipids were measured directly in this phase by inorganic PO_4 assay following perchloric acid hydrolysis (Bartlett, 1959). Individual Ch, FA, MG, and DG were separated by thin-layer chromatography and quantified by scanning thin-layer densitometry (Bitman & Wood, 1981; Bitman et al., 1981). Plates were first channeled with a preadsorbent zone [Si 250-PA (19C), Baker Chemical Co., Phillipsburg, NJ] and washed in $(C_2H_5)_2O$. Microliter samples of lipids were applied to the plates by means of calibrated capillary tubes (Drummond Scientific Co., Broomall, PA).

Plates were developed first in $CHCl_3/CH_3OH$/glacial CH_3COOH (98:2:0.1 v/v/v) and, after drying under N_2 for 15 min, were redeveloped in $C_6H_{14}/(C_2H_5)_2O$/glacial CH_3COOH (94:6:0.2 v/v/v) (Bitman et al., 1981). Plates were then stained by dipping for 3 s in 10% (w/v) $CuSO_4$ dissolved in 8% (v/v) H_3PO_4. To standardize spot densities, plates were charred in a gas–liquid chromatograph oven (Shimadzu Model GC-9A, Columbia, MD), with a temperature program that increased from 50 to 180 °C at a heating rate of 10 °C/min. Within 1 h following charring, the separated lipid spots were quantified by linear densitometry at 370 nm using a dual-wavelength TLC scanner (Shimadzu Model CS-930). Quantitation of each lipid class was estimated from standard curves by employing a range (0.5–25 μg) of pure standards cochromatographed in the same solvent systems. Standard densitometric curves, plotting spot density versus lipid mass, were linear ($r \geq 0.95$) and were reproducible to within ±10%.

Freeze-Fracture Electron Microscopy. Small portions (1–4 μL) of equilibrated aqueous lipid mixtures were sandwiched between thin disks of >99% pure copper at 37 °C and frozen in the liquid phase of partially solidified propane: Specimens were subsequently stored in liquid N_2 and then fractured at −105 °C in a Balzers 300 freeze-etch apparatus employing a double-replica attachment (Madara, 1983). Specimens were replicated with platinum–carbon at 45 °C, cleaned in 3 M HNO_3 and subsequently washed in and floated on pure H_2O, and "picked up" on formvar-coated 200-mesh grids. Replicas were examined and photographed with a Philips 300 electron microscope (Philips Electronic Instruments, Mahwah, NJ).

Potentiometric Titrations. Five milliliters of 1 g/dL aqueous MBS/MIL mixtures (molar ratios 100:0, 75:25, 50:50, 25:75, 0:100) were prepared in 0.15 M NaCl without buffer, as described above. Following addition of a few microliters of 2 M NaOH to elevate their pH values to ~11, the mixtures were vortex-mixed and placed in the glass cup of a manual titration assembly (TTT1, Radiometer, Copenhagen, Denmark). Proton titrations were carried out with 2 M HCl at 23 °C by a manual equilibrium method that included continuous magnetic stirring under circulating H_2O-saturated N_2 (Small, 1971; Igimi & Carey, 1980). Following sequential additions of 1–2 μL of 2 M HCl by means of a Hamilton syringe, the pH values were monitored continuously with a Radiometer glass electrode until an equilibrium value to two significant figures was attained. Each mixture was also inspected visually with the aid of a high-intensity light source, and appearances were recorded. Because of extremely slow equilibration times, the consumption of an approximate equivalent of HCl to bring the final pH value from ~11 to 2–3 required at least 8–24 h and sometimes longer. The pK'_a values of the conjugated BS mixture and of FA in micellar phase mixtures were calculated as described (Small, 1971; Igimi & Carey, 1980; Hofmann, 1968). For samples with relative lipid compositions outside the micellar zone, the ionization state in the physiological pH range (pH 5.5–7.5) was estimated on the basis of proton titration curves of pure aqueous Na FA and K FA systems (Shankland, 1970; Small, 1986; Cistola et al., 1988).

Concentrations of Monomeric MBS. Monomeric MBS concentrations at 37 °C were determined for three MBS:MIL ratios (no Ch) at equilibrium (1 g/dL, pH 6.5). The cmc of a pure MBS system (no added MIL) was estimated by the spectral shift of 2.5×10^{-6} M Rhodamine 6G (Carey & Small, 1969). To assess the intermicellar BS concentration (imc) at the micellar phase boundary of the MBS/MIL system, the technique of Mazer and colleagues (Mazer et al., 1980) was employed, wherein a plot of [MBS] as a function of [MIL] at the micellar phase boundary for total lipid concentrations of 0.25, 0.5, 1.00, 2.5, and 5.0 g/dL was extrapolated to a positive intercept on the MBS axis. To estimate the monomeric MBS concentration in the one-phase liquid-crystalline zone at equilibrium, three lipid mixtures plotting within this region were ultracentrifuged for 24 h at 100000*g*. The harvested optically clear subphases were shown to be free of mixed micelles and liquid-crystalline vesicles by QLS (no autocorrelation function) and were assayed enzymatically for MBS.

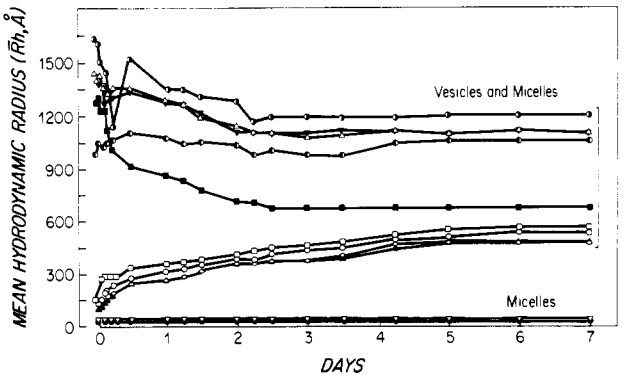

FIGURE 1: Equilibration rates at 37 °C of continuously shaken 1 g/dL mixtures of coprecipitated mixed bile salts (MBS) (composition as in Table I), mixed intestinal lipids (MIL) (composition A of Table II), and no cholesterol (CH) following addition of buffered aqueous solvent (pH 6.5). Mean hydrodynamic radii ($\bar{R}_h$, in angstroms) were measured by quasielastic light scattering (QLS). Two mixtures with relative compositions falling within the micellar zone equilibrated before the first QLS measurement was made (30 min); other mixtures with compositions lying within the two-phase mixed micelle plus vesicle zone (see Figure 2) equilibrated slowly and in two distinct patterns (discussed in text). MBS:MIL molar ratios: 20:80 (◑); 25:75 (◐); 30:70 (▼); 35:65 (△); 40:60 (■); 45:55 (□); 50:50 (○); 55:45 (▲); 58:42 (◇); 65:35 (▽); 70:30 (●).

Results

Proof of Equilibration. Observed with the unaided eye, the gross physical states of most mixtures changed markedly during the first 4 days of observation; thereafter, the changes were slight or nonexistent, indicative of equilibration (~4–7 days). More refined QLS analysis of equilibration rates, for a systematic series of 1 g/dL mixtures of MBS and MIL at 37 °C (pH 6.5), yielded the results displayed in Figure 1. The $\bar{R}_h$ values (angstroms), plotted as functions of time (days), show that lipid mixtures with the highest MBS:MIL ratios attained equilibrium sizes ($\bar{R}_h < 40$ Å) before the first QLS measurement was made and were consistent with mixed micelles (Figure 1). The $\bar{R}_h$ values of mixtures with intermediate-to-low MBS:MIL ratios (shown below to be composed of unilamellar vesicles and mixed micelles) were dominated by the scattering from the larger particles and demonstrated two different phenomena: with passage of time samples with MBS:MIL ratios just beyond the micellar phase limit displayed a continuous and curvilinear *increase* in $\bar{R}_h$ values, reaching equilibrium sizes after 5 days, while mixtures with the lowest MBS:MIL ratios showed a time-dependent *decrease* in $\bar{R}_h$ values, reaching equilibrium sizes at 3–4 days. For construction of the ternary phase diagram, equilibration times for all systems with binary or ternary lipid components were ≥7 days.

Condensed Ternary Phase Diagram. The condensed phase diagram for the three-component MBS/MIL (composition A in Table II)/Ch system at 1% w/v in 0.15 M aqueous Na^+ (pH 6.5, 37 °C) is displayed on triangular coordinates in Figure 2. As depicted in Figure 2 (inset), the phase diagram

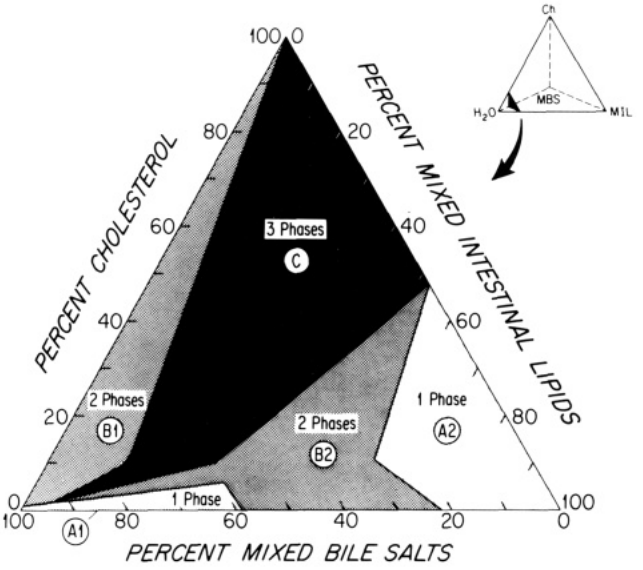

FIGURE 2: Equilibrium phase diagram of the MBS–MIL–Ch system (1 g/dL total lipids, pH 6.5, 37 °C; MIL composition, mixture A of Table II) plotted on triangular coordinates. The main diagram represents a cut at 99% H_2O of the quaternary MBS–MIL–Ch–H_2O phase diagram represented by the regular tetrahedron in the inset. For pictoral clarity, the cut (solid black) in the inset is shown at reduced percent H_2O. In the triangular phase diagram, the one-phase zones (A_1) and (A_2) are composed of micellar and lamellar liquid-crystalline phases, respectively. Two-phase zone B_1 is composed of Ch-saturated micelles and Ch crystals. Two-phase zone B_2 contains Ch- and MIL-saturated mixed micelles and unilamellar vesicles of MIL saturated with MBS but not saturated with Ch. The three-phase zone (C) contains Ch-saturated micelles, lamellar liquid crystals, and Ch monohydrate crystals (described fully in text).

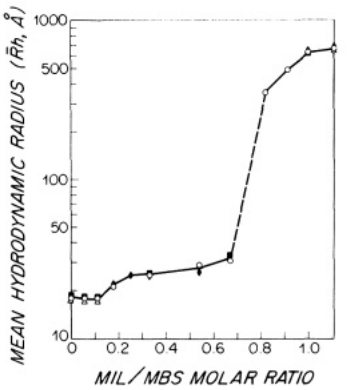

FIGURE 3: Dependence of mean hydrodynamic radius ($\bar{R}_h$, in angstroms) of lipid particles upon increases in MIL:MBS molar ratio at four constant Ch contents. Mole percent Ch are 0 (○), 1 (△), 2 (■), and 3 (◆). Increases in MIL:MBS ratio are equivalent to points falling from left to right along, or parallel to, the base axis of the triangle (Figure 2), i.e., progressing across the micellar phase (A_1) into the two-phase (B_2) zone. Increases in mole percent Ch content therefore represent compositions inside the triangle (Figure 2) extending from the base axis toward the Ch apex. With increases in MIL:MBS ratio, there is a sigmoidal increase in micellar $\bar{R}_h$ values from pure MBS = 18 Å (no MIL) to 32 Å at a MIL:MBS ratio of ~0.7. Between MIL:MBS ratios of 0.8 and 1.2 the vesicles in zone B_2 dominate the QLS light scattering intensity, and the $\bar{R}_h$ values range from 350 to 600 Å. Ch contents between 0 and 3 mol % show no appreciable influences on either micelle or micelle plus vesicle sizes. (Other conditions as in legend to Figure 2.)

represents a cut at 99% H_2O (v/w) of the quaternary MBS/MIL/Ch/H_2O system to represent a typical postprandial aqueous lipid concentration in the upper small intestine of adult human beings. An apex of the triangle represents the phase behavior of 100% of each component: MBS (left apex); Ch (top apex); and MIL (right apex). The sides of the triangle represent the phase behavior of binary mixtures of components, and the triangle itself represents the phase behavior of ternary mixtures of all three components in buffered aqueous solvent.

As shown by the intersections on the base axis, ~22 mol % MBS was soluble in the single lamellar liquid-crystalline phase of MIL; at 58 mol % MBS there was another phase boundary where the single isotropic MBS/MIL micellar phase was entered. On the left axis, the phase boundary at ~1–1.5 mol % Ch represents the maximum equilibrium solubility of Ch in MBS micelles. At higher Ch contents, the systems separated into two phases composed of Ch-saturated micelles and Ch monohydrate crystals. On the right-hand axis, the phase boundary at ~50% MIL and 50% Ch represented the maximum solubility of Ch in the lamellar liquid-crystalline phase of MIL. At higher Ch contents, Ch monohydrate crystals separated from this phase to form a two-phase system.

Five distinct zones were identified within the phase diagram. Two were one-phase zones (A_1, A_2), composed of pure micellar (A_1) and lamellar liquid-crystalline (A_2) phases, respectively. Two were two-phase zones (B_1, B_2), composed of Ch-saturated micelles plus Ch crystals (B_1) and Ch-plus-MIL-saturated micelles and unilamellar vesicles (B_2), respectively. There was a single three-phase zone (C), composed of Ch-saturated micelles containing little MIL, Ch monohydrate crystals, and lamellar MIL liquid crystals saturated with Ch. According to Gibbs phase rule (see Theoretical Considerations), at constant temperature and pressure, the three-phase zone was invariant; therefore, the composition of each coexisting phase is given by the point apexes of the zone (Figure 2).

Single-Phase Zone A_1: The Micellar Phase and Its Boundaries. As displayed in Figure 3, with increasing MIL:MBS ratio within the micellar zone, micellar $\bar{R}_h$ values were initially constant at approximately 18 Å. With further increases in MIL:MBS ratio, $\bar{R}_h$ values increased to 26 Å and then gradually reached 32 Å. With further increases in MIL:MBS ratio, the micellar phase boundary was crossed (see Figure 2), and an abrupt increase in $\bar{R}_h$ values to those typical of vesicles (~400 Å) occurred at an MIL:MBS molar ratio of >0.68 (Figure 3). From these and other results (see below), it was apparent that binary or ternary lipid mixtures containing only mixed micelles produced a single particle size distribution ($V < 30\%$) with $\bar{R}_h$ values ≤40 Å that did not diverge in size as the micellar phase limit was approached. Under high-intensity illumination, visual inspection of each set of equilibrated mixtures with compositions falling both inside *and* outside the micellar phase boundary revealed that they were optically clear. A bluish opalescence (Tyndall phenomenon) did not appear in any lipid mixture until well beyond the QLS-determined micellar phase boundary. With further increases in MIL:MBS ratio, the Tyndall phenomenon increased in intensity, finally changing to cloudiness when one-phase zone A_2 was entered. Figure 3 also shows that the influences of low concentrations (1–3 mol %) of solubilized Ch on micelle and micelle-plus-vesicle sizes were negligible.

Figure 4 displays $\bar{R}_h$ values for mixtures with relative lipid compositions falling within the two-phase B_2 zone (top) and the one-phase A_1 zone (bottom) (see Figure 2) as functions of increases in mole percent Ch. As shown by the series of curves at the top of Figure 4, there was no systematic influence of solubilized Ch on $\bar{R}_h$ values of the particles in the two-phase zone (B_2), which represented principally the $\bar{R}_h$ values of vesicles. As shown by the set of curves at the bottom (Figure 4), up to 2 mol % Ch was solubilized in the micellar phase at molar MBS:MIL ratios of 100:0 and 90:10 without an appreciable change in $\bar{R}_h$ values. Further additions of Ch resulted in the separation of Ch monohydrate crystals (not displayed).

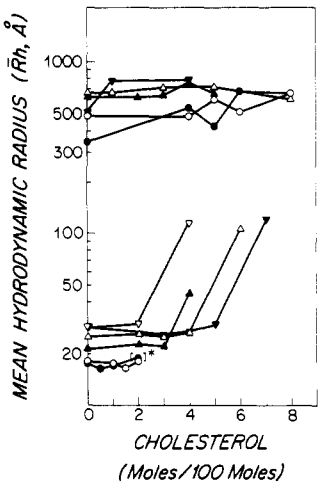

FIGURE 4: Mean hydrodynamic radius ($\bar{R}_h$, in angstroms) of lipid particles in micellar zone (A_1) and micelle plus vesicle zone (B_2) as functions of mole percent Ch content for systematic variations in MBS:MIL ratio. For upper data set, MBS:MIL ratios are 45:55 (▼), 48:52 (△), 50:50 (▲), 53:47 (○), and 55:45 (●). For lower data set, MBS:MIL ratios are 60:40 (▽), 65:35 (▼), 75:25 (△), 85:15 (▲), 90:10 (○), and 100:1 (●). At the two highest MBS:MIL ratios (100:0, 90:10), Ch content influenced micellar size neither within the micellar zone nor with extension into metastable supersaturation (2 mol % Ch). With MBS:MIL ratios between 85:15 and 60:40, the sizes of micelles were also invariant with Ch content; however, the steep upslope in $\bar{R}_h$ values at the highest Ch contents exceeds micellar solubility and represents extension into the B_2 zone, where a coexistence of vesicles and micelles was present (see Figure 2). Curves in the upper part of the figure (for compositions in two-phase zone B_2) show that the $\bar{R}_h$ values, which principally represent vesicle sizes, were also independent of Ch content. However, notable variations in vesicle sizes occurred with decreases in MBS:MIL ratio at constant mole percent Ch. (Other conditions as in legend to Figure 2.)

With progressively lower MBS:MIL ratios, solubilized Ch had, at first, no influence on $\bar{R}_h$ values, but with higher Ch contents, an abrupt increase in $\bar{R}_h$ values to >100 Å was indicative of vesicles. This phenomenon marked entrance into a sliver of the two-phase region that overlay the upper boundary of the micellar phase (B_2 in Figure 2), where small unilamellar vesicles, but no Ch crystals, coexisted with saturated mixed micelles. Because it was possible, at metastable supersaturation (Figure 4), to solubilize ~2 mol % Ch in 1 g/dL pure MBS (no MIL, pH 6.5), the equilibrium Ch solubility was estimated by analysis to lie between 1 and 1.5 mol %. As verified by the lower curves in Figure 4, progressive decreases in the MBS:MIL ratio led to progressive increases in Ch solubility, to a maximum of 5 mol % Ch at an MBS:MIL ratio of ~65:35, falling again to 2 mol % at a ratio of 60:40 and to zero at the micellar phase limit, all reflecting the shape of the micellar phase boundary (Figure 2). The cmc of the pure MBS system (no MIL or Ch) by the Rhodamine 6G method was ~1.34 mM, whereas the extrapolated imc value at the micellar phase limit (see Methods) was 3.5 mM.

Parts A and B of Figure 5 depict the proton titration curves of 1 g/dL 100% MBS and 1 g/dL MBS:MIL (75:25 mol/mol), respectively, both compositions plotting within the micellar phase. With pure MBS (Figure 5A), the titration was initiated at inflection point W (pH ~8.0) and was completed at inflection point Z (pH ~3.0), indicating that the taurine-conjugated bile salts were not titrated by HCl (Small, 1971; Carey, 1983). The calculated equivalence between the moles of HCl consumed and the moles of glycine-conjugated BS in the mixture (Table I) was 98%. Precipitation of the undissociated glycine conjugates occurred at pH 3.83 (point Y, Figure 5A)—approximately 1 pH unit lower than for pure glycine-conjugated BS (Small, 1971), presumably because of

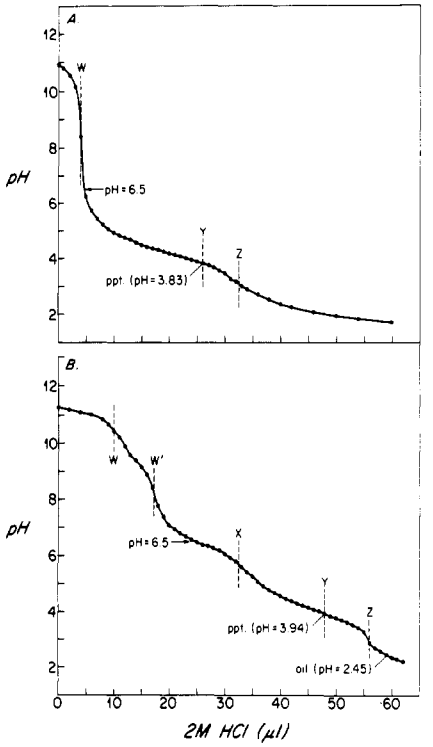

FIGURE 5: Proton titration curves of 1 g/dL mixtures with MBS:MIL (composition A, Table II) molar ratios of 100:0 (A) and 75:25 (B). In (A), the glycine-conjugated, but not taurine-conjugated, bile salts (BS) were titrated between pH ~8.5 (W) and pH ~3.2 (Z); the precipitation point occurred at pH 3.83 (Y). The calculated pK'_a of the MBS mixture was 4.3 (Small, 1971). In (B), both FA (of MIL) and glycine-conjugated BS (of MBS) were sequentially titrated. Between pH 10.2 and pH 8.3 (W → W_1) the micelles formed by ionized FA soaps were titrated. Between W_1 and X (pH ~6) the "acid soap" complex of FA was titrated together with some MBS. Between X and Y (pH ~4.2) titration of FA plus MBS was not distinguishable. Crystal precipitation at pH 2.94 was due to protonated glycine-conjugated bile acids, and precipitation at pH 2.45 was caused by undissociated FA "oils" (see text for further details).

the presence of taurine-conjugated BS. The mean pK'_a of the glycine conjugates, calculated by the formula of Back and Steenberg (1950), was 4.3; hence, over the pH range 7.5, 6.5, and 5.5, <0.1, <1, and <10% of the glycine conjugates were undissociated, respectively. In Figure 5B, between pH 10.5 (W) and 3 (Z), both FA (of MIL) and glycine-conjugated BS of the MBS were titrated. An analysis of this curve (Shankland, 1970; Small, 1986; Cistola et al., 1988), and the stoichiometry at precipitation point Y, suggested that titration of ionized FA was initiated before glycine-conjugated BS. The shape of the curve in the middle range of pH values suggested that the pK'_a of FA in the MBS micelles was ~6.5 and therefore existed predominantly as a 1:1 acid soap (Cistola et al., 1988). The precipitation pH at Y (3.94) was comparable to that of pure MBS (Figure 5A), giving a calculated pK'_a of 4.4 for the glycine conjugates, indicating that 99% of glycine conjugates were ionized within the mixed micellar phase at pH 6.5. FA "oils" only became visible within this system at pH 2.45 (Figure 5B).

Single-Phase Zone A_2. Beyond a MBS:MIL molar ratio of ~22:78 (Figure 2), the single-phase region (A_2) was identified by polarizing microscopy as containing lamellar liquid crystals (37 °C, 0.15 M Na^+, pH 6.5). When subjected to prolonged high-speed ultracentrifugation (centrifugal force × time = 3×10^8 g·min), this zone produced a floating liquid-crystalline phase with $\bar{R}_h$ values ≫5000 Å and a subphase devoid of micellar or vesicle particles, as inferred from its inability to develop a QLS autocorrelation function. By BS

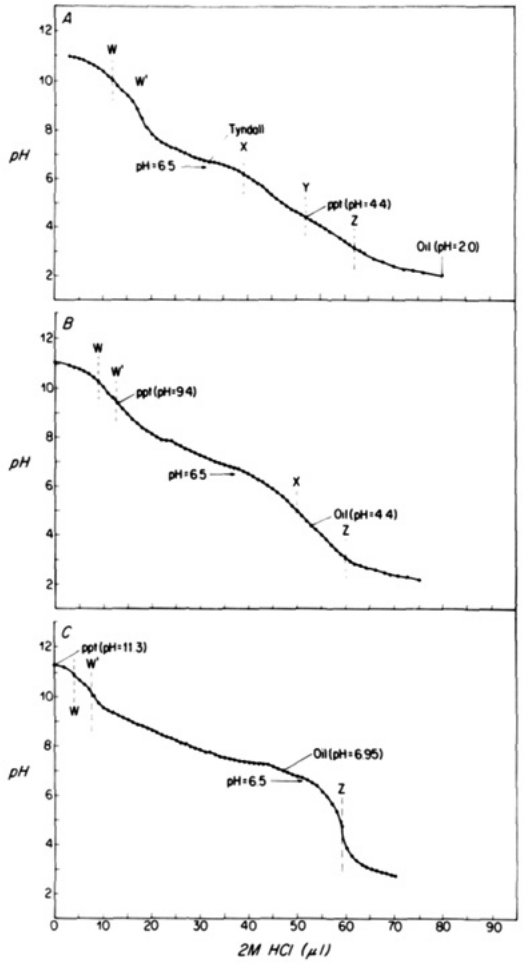

FIGURE 6: Proton titration curves of 1 g/dL MBS:MIL mixtures with molar ratios of 50:50 (A), 25:75 (B), and 0:100 (C). In (A), between W and W′ the soap micelles of ionized FA were titrated. Between W′ and X acid soaps of FA plus MBS were titrated. The Tyndall phenomenon at pH ~6.5 heralded the onset of spontaneous vesicle formation by acid soaps, as verified by QLS. Between X and Y, FA and MBS were titrated, and the precipitation point for glycine-conjugated bile acids was at pH 4.4. The FA plus MBS titration was complete at Z, and FA oils were identified first at pH 2.0. In (B), because of the lower MBS:MIL ratios, all of the phenomena in (A) are shifted upward to higher pH values. In particular, the pH values of the acid soap range extended from W′ (pH ~9.4) to X (pH ~5.5); undissociated FA oils appeared at pH 4.4. In (C), pure FA (with small amounts of added PL, MG, and DG and no MBS) was titrated. Because turbidity was present at pH 11.3, it is obvious that the ionized micellar Na^+ FA concentration was insufficient to solubilize the PL, MG, or DG in the MIL mixture which separated as a precipitate of unidentified physical state. Between W and W′ the FA in the ionized micelles was titrated. However, between W′ (pH 10.5) and the formation of FA oils at pH 6.95, acid soaps were titrated. Between pH 6.95 and Z, FA were further titrated and precipitated continuously as undissociated FA oils (further discussed in text).

analysis, the subphase contained a monomeric BS concentration of 2.1 ± 0.1 mM (n = 3). Systems within the A_2 zone at pH 6.5 that contained FA:MG molar ratios of 10:1 and 20:1 in the MIL (Table II) formed floating lenses of FA oils (Figure 2), whereas, at pH 5.5, the floating FA oils comprised ~2–5% of sample volume. However, at pH 7.5, when the FA was more completely ionized, we detected no FA oil phase, and only a single lamellar liquid-crystalline phase (in equilibrium with MBS monomers), in this zone.

Parts B and C of Figure 6 display the proton titration curves for MBS:MIL molar ratios of 25:75 (i.e., near the phase limit of zone A_2) and 0:100, where only pure MIL, and no MBS, were present (Figure 2). In Figure 6B, the system showed an initial precipitation at pH 9.4 which, by analogy with other

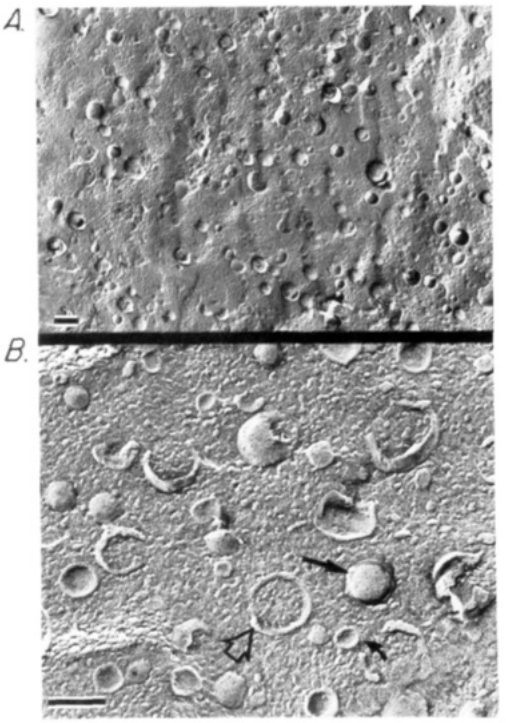

FIGURE 7: Electron photomicrograph of a freeze-fracture replica of a mixture falling within the B_2 zone (Figure 2) at low (A) and high (B) magnification. Black bars represent 1000 Å. In both photomicrographs, the vesicles are unilamellar (arrows point to bilayers and freeze-fractured surfaces) and of heterogeneous size (radii 150–600 Å). The coexisting mixed micelles in the samples (see Figure 2) were not visualized by this technique (conditions: 1 g/dL, pH 6.5, initial temperature 37 °C, MIL composition as in A of Table II).

work (Shankland, 1970; Small, 1986; Cistola et al., 1988), heralded the precipitation of the 1:1 lamellar acid soap of FA from ionized NaFA soap micelles. With continued addition of HCl, acid soap continued to precipitate from the mixtures down to pH 7.9. From pH 7.9 until an unidentified oil appeared at pH 4.4, this system was very complex, containing lamellar acid soaps, protonated FA, and protonated glycine-conjugates of the MBS, all possibly coexisting with other unidentified phases, which could be inverted cubic, hexagonal, or micellar systems (Small, 1986). In the pure MIL mixture (Figure 6C), the system was grossly cloudy at pH 11.3, indicating that the concentration of ionized FA soaps in the MIL mixture was insufficient to solubilize the MIL's MG, PL, and DG content as mixed micelles (Table II, composition A). Continued titration with HCl increased the turbidity of the system until an oil phase separated at pH 6.95. Within the pH range studied by phase equilibria methods (pH 5.5–7.5), the *pure* MIL system (right apex of Figure 2) apparently formed FA oil, 1:1 acid soap, and presumably other unidentified phases [see Small (1986) and Cistola et al. (1988)].

Multiphase Zones of the Phase Diagram. The two-phase zone designated B_1 (Figure 2) contained Ch monohydrate crystals dispersed in an isotropic micellar phase at equilibrium. (The metastable phase diagram was not examined for the transient presence of Ch-rich vesicles.) The Ch crystals were rapidly pelleted by low-speed centrifugation (see Methods), and, by lipid analysis, the isolated micellar phase was saturated with Ch (not displayed). The two-phase zone (B_2) of the phase diagram (Figure 2) contained unilamellar lipid vesicles in equilibrium with a saturated mixed micellar solution. Figure 7 shows a typical freeze-fracture electron micrograph of an MIL/MBS mixture in the B_2 zone, demonstrating that the vesicles were, indeed, unilamellar only. The diameters of the vesicles were markedly heterogeneous, varying in radii from

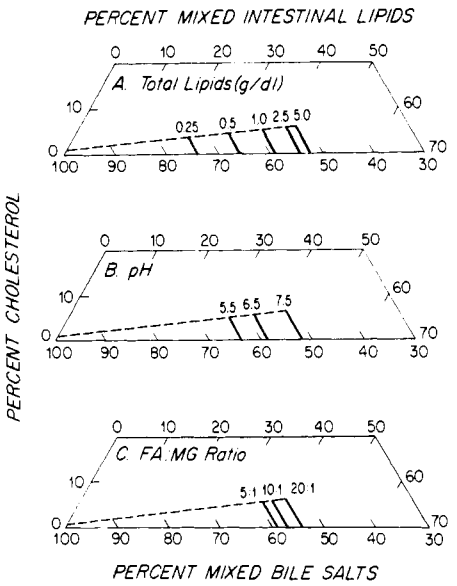

FIGURE 8: Influence of physical–chemical variables of physiological importance of the micellar phase boundary (Figure 2), i.e., between the pure micellar phase (A_1) and the vesicle-plus-micelle zone (B_2). Panel A shows enlargement of the micellar zone with increases in total lipid concentration [0.25–5 g/dL, composition A (Table II), 37 °C, pH 6.5]. Panel B shows enlargement of the micellar zone with increases of pH [5.5, 6.5, 7.5, composition A (Table II), 37 °C, 1 g/dL]. Panel C shows enlargement of the micellar zone with increasing FA:MG ratio [5:1, 10:1, 20:1, compositions A, B, C, respectively (Table II), 37 °C, pH 6.5]. Higher total lipid concentrations, pH, and FA:MG ratios all independently extended the size of the micellar zone (further discussed in text).

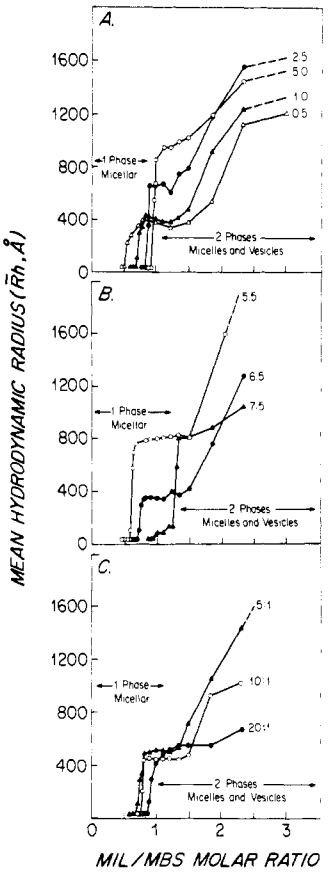

FIGURE 9: Influence of physical–chemical variables on equilibrium phase limits and vesicle sizes ($\bar{R}_h$, in angstroms) of B_2 zone (Figure 2) as functions of MIL:MBS ratio (no Ch). Displayed are variations in (A) total lipid concentration, (B) pH, and (C) FA:MG ratio. The vesicle sizes are larger with higher total lipid concentrations (A), lower pH (B), and lower FA:MG ratio (C) (further discussed in text).

150 to 600 Å compared with the 1000-Å bar, but no particles of micellar size (radii ≤ 40 Å) were resolved in any electron micrograph. Further, no FA oil phase separated with any phase equilibria composition or condition within the B_2 zone, including an MIL mixture containing a FA:MG ratio of 20:1 at pH 5.5.

Figure 6A displays the proton titration curve for a 50:50 MBS:MIL mixture, whose relative composition plotted within the B_2 zone at pH 6.5. Proton titration was initiated at point W, followed by a sharp inflection point at W′. When the pH was further lowered, the system remained optically clear but, at pH 6.7, a Tyndall phenomenon (but no precipitation) appeared. By QLS, only micelles ($\bar{R}_h$ < 40 Å) were present between pH 11.4 and 6.7, indicating that the micellar phase boundary extended to at least this lipid ratio. With all lower pH values, the Tyndall phenomenon intensified, indicating the continuation of spontaneous vesicle formation, as verified by QLS ($\bar{R}_h$ > 200 Å); flocculent precipitation occurred at pH 4.4, and with further decreases in pH, FA oils were detected at pH 2.

The three-phase zone (C, Figure 2) contained a mixture of saturated mixed micelles, Ch monohydrate crystals, and lamellar liquid crystals, all of invariant composition (Carey, 1983), indicated by the point apexes of this zone (Figure 2).

Physical Chemistry of the Micellar Phase Boundary. Figure 8 depicts the effects of increasing total lipid concentration, pH, and FA:MG ratio on the relative lipid compositions of the right-hand boundary of the micellar phase. A 20-fold increase in total lipid concentration (0.25–5.0 g/dL, composition A, Table II) produced incremental increases in the width of the micellar phase by ~22 mol % MIL (Figure 8A). This principally reflected the magnitude of the imc (~3.5 mM) of the MBS/MIL system, which is maintained approximately constant with varying total lipid concentration [cf. Mazer et al. (1980)]. As shown in Figure 8B, and expected on the basis of the proton titration curves (Figure 6A), an increase in pH values by 3 units (composition A, Table II, 1 g/dL total lipid) progressively expanded the micellar phase limit by ~12 mol % MIL. Figure 8C demonstrates that, at constant pH and total lipid concentration (pH 6.5, 1 g/dL total lipid), a 4-fold increase in the FA:MG molar ratio of the MIL mixture (Table II) induced only a small expansion (~5 mol % MIL) of the micellar phase.

Physical Chemistry of Lipid Particles in the Physiological (B_2) Zone. Figure 9 displays equilibrium $\bar{R}_h$ values by QLS as functions of increasing MIL:MBS molar ratios for mixtures with relative lipid compositions falling within the micellar zone (zone A_1, Figure 2) and extending across the right-hand micellar phase boundary into zone B_2 (Figure 2), where micelle-plus-vesicle phases coexisted. These measurements were carried out systematically for variations in total lipid concentration (Figure 9A), pH (Figure 9B), and FA:MG ratio (Figure 9C), all in the absence of Ch. Just inside the micellar zone, $\bar{R}_h$ values were <40 Å and changed only slightly with increases in MIL:MBS ratio (see Figure 3). As the micellar phase boundary was crossed, abrupt increases in $\bar{R}_h$ values occurred over very narrow MIL:MBS ratios, except in the case of pH 7.5 (Figure 9B), where a stepwise increase in size was noted and verified (n = 4). Further increases in MIL:MBS ratios invariably led to a plateau or gradual increase in $\bar{R}_h$ values, followed by nearly linear increases in particle sizes to a maximum of 1600 Å, the size limit accurately resolvable of QLS. This is consistent with enlarging vesicle sizes, since, in the measurement of $\bar{R}_h$ values, the light scattering signal from vesicles dominated that from coexisting micelles (Cohen,

Table III: Dissolution of Unilamellar Vesicles plus Saturated Mixed Micelles (B_2 Zone) by Unsaturated Mixed Micellar Solutions (A_1 Zone): Compositions, Sizes, and Kinetics[a]

	unsaturated "solvent" phase			saturated "phase"				
	mixed micelle composition			mixed micelle plus vesicle composition				
mixture	molar ratio MBS:MIL	mol % Ch	initial $\bar{R}_h$ (Å)	molar ratio MBS:MIL	mol % Ch	initial $\bar{R}_h$ (Å)	equilibrium micellar $\bar{R}_h$ value (Å)	time to attain equilibrium micellar $\bar{R}_h$ value (min)
A[b]	95:5	1.5	29	50:50	3	653	30	3
B	95:5	1.5	29	60:40	4	539	35	4
C	95:5	1.5	29	55:45	0	675	37	10
D[b]	85:15	2	31	50:50	3	653	30	11
E	75:25	2	34	50:50	3	653	42	11
F[b]	75:25	2	34	50:50	3	653	43	12
G[b]	65:35	4	35	50:50	3	653	40	48

[a] Three hundred microliters of unsaturated mixed micellar solutions was mixed with equal volumes of saturated mixed micelle plus unilamellar vesicle solutions. Conditions: FA:MG ratio 5:1; pH 6.5; 1 g/dL final concentration; T = 37 °C. Systems were vortex-mixed at time zero for 30 s prior to QLS analysis. [b] The decay in $\bar{R}_h$ values as functions of time for these systems is plotted in Figure 12.

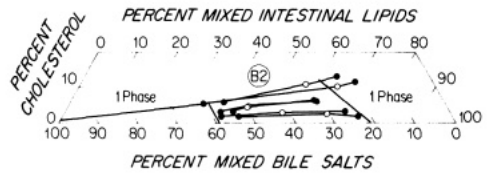

FIGURE 10: Truncated triangular phase diagram to show tie-lines of the B_2 zone (of Figure 2). Overall relative lipid composition of mixtures in the B_2 zone are shown (open symbols) together with relative lipid compositions of the constituent micellar (left side) and vesicle (right side) phases (solid symbols) following ultracentrifugal separation and analysis. The tie-lines connecting the compositions of the coexisting phases slope progressively upward to the right with increasing Ch content. Within experimental error, the relative lipid compositions of the constituent micelles approximate the micellar phase boundary, while the relative lipid compositions of the constituent vesicles approximate the one-phase liquid-crystalline boundary (see text for details).

1986). Parts A–C of Figure 9 show that increases in total lipid concentration from 0.5 to 5.0 g/dL, reduction in pH from 7.5 to 5.5, and a diminution in FA:MG ratio (20:1 to 5:1) led to systematic increases in vesicle sizes in the two-phase (B_2) zone.

Tie-Lines of the B_2 Zone. Tie-lines for the individual phases in the two-phase zone (B_2) were analytically delineated following ultracentrifugal separation and analysis (see Methods) for six MBS/MIL mixtures (MIL composition A Table II, 1 g/dL, pH 6.5). Figure 10 shows the relative lipid compositions of the 12 separated phases (solid symbols) and the 6 original mixtures (open symbols) plotted on truncated triangular coordinates (same axes as Figure 2). The relative lipid compositions of the constituent phases plotted on, or close to, the micellar and liquid-crystalline phase boundaries, respectively, and, within experimental error, the tie-lines connecting the relative compositions of the separated phases and the original mixtures were linear. The tie-lines verify that not only was the B_2 zone composed of two phases (micelles and vesicles) but, in addition, the micelles were saturated with MIL and Ch, and the liquid crystals (vesicles) were saturated with MBS. As mole percent Ch increased, the tie-lines became less parallel to the base line and sloped upward to the right, indicating that the single liquid-crystalline phase solubilized more Ch than the micellar phase (see Figure 2).

Multicomponent QLS Analysis. Figure 11 displays two- and three-component curve-fitting analysis of QLS autocorrelation functions (Cohen, 1986) for four mixtures with relative lipid compositions within the two-phase (B_2) zone. The middle of the figure shows relative proportions of lipid particles by number and mass ratio, and the bottom histograms show the individual intensities of scattered light, as well as the derived R_h values of micelles and vesicles. Sample A, with a

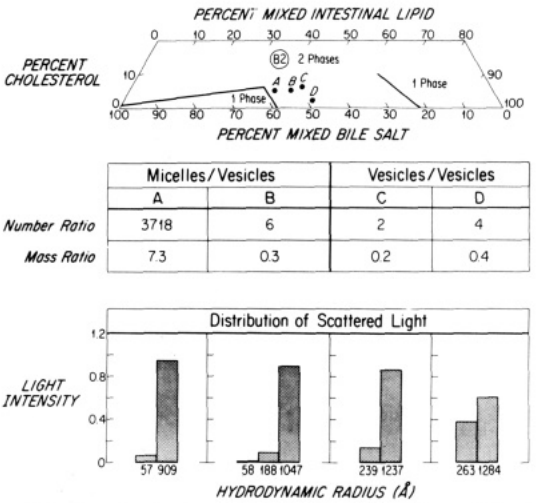

FIGURE 11: Truncated triangular plot (top) as in Figure 2 to display four MBS–MIL–Ch mixtures, with relative lipid compositions falling within the B_2 zone (Figure 2). For each relative composition, the middle panels show number and mass ratio of micelles to vesicles and vesicles to vesicles by multicomponent QLS analysis. The bottom bar graphs display light intensities and individual R_h values of micelles and vesicles (A, B) and two-vesicle populations (C, D) in the B_2 zone (see text for further details).

MBS:MIL ratio of 60:40 and 5 mol % Ch, contained micelles with an R_h value of ~57 Å[5] and vesicles with an R_h value of 909 Å. Sample B, with a MBS:MIL ratio of 55:45 and 5 mol % Ch, contained micelles with an R_h value of ~58 Å[5] and two populations of vesicle particles with R_h values of 188 and 1047 Å, respectively. Samples C and D, with MBS:MIL ratios of 53:48 and 50:50 and 6 and 2 mol % Ch, respectively, were analytically resolved by QLS for two vesicle populations with R_h values of 239 and 263 and 1237 and 1284 Å, respectively. Although the fractions of light intensity scattered by the micellar components in mixtures A and B were $<^1/_{20}$ of the overall scattering, nevertheless, as indicated by the numerical ratios, micelles constituted the majority of particles present. Further, when all mixtures (A–D) were ultracentrifuged, a thin liquid-crystalline phase separated and QLS of all isotropic subphases gave $\bar{R}_h$ values of ~60 Å, indicating that micelles indeed coexisted with vesicles in all four mixtures, although, in mixtures C and D, micelles were not analytically resolved by multicomponent QLS analysis.

[5] Whereas systematic QLS examination of pure micellar phases in these systems revealed that the upper limit for micellar $\bar{R}_h$ values was ≤40 Å, these *derived* R_h values for saturated micelles in the B_2 (two-phase) zone are likely to be overestimates due to the high intensity of light scattered from coexisting unilamellar vesicles (Cohen, 1986).

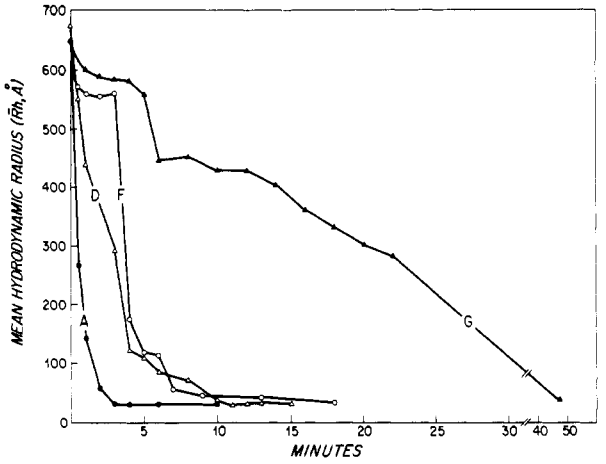

FIGURE 12: Dissolution rates of vesicles in model systems of the B_2 zone (Figure 2) as functions of the solvent (unsaturated mixed micellar solutions from the A_1 zone) composition (letter codes as in Table III). When the MBS micellar phase was appreciably unsaturated with MIL (curves A, D, and F), vesicle dissolution was very rapid (5–10 min). However, when the micellar phase was near saturation with MIL, dissolution was slow (curve G).

Vesicle Dissolution by Unsaturated Micelles. Table III lists relative lipid compositions, initial and final particle sizes ($\bar{R}_h$ values), and equilibration times for dissolution of MBS/MIL/Ch mixtures from zone B_2 by unsaturated micellar mixtures with relative MBS/MIL/Ch compositions falling within zone A_1. Initial compositions of the vesicle-containing samples were similar to those reported for aqueous intestinal lipids during established fat digestion and absorption (Carey et al., 1983; Hernell et al., 1990). As demonstrated by representative time-dependent plots of $\bar{R}_h$ values in Figure 12, when mixed micellar phases were very unsaturated with MIL (curves A, D, and F and Table III), rapid dissolution of unilamellar vesicles of the B_2 zone (Figure 2) occurred within 3–12 min to produce pure micellar solutions, all plotting within the A_1 zone (Figure 2). In contrast, when the mixed micellar solutions were more enriched with MIL (Table III and curve G, Figure 12), dissolution rates of B_2 zone mixtures to attain equilibrium micellar sizes approximating those at the phase limit ($\bar{R}_h \sim 40$ Å) were appreciably slower ($\sim$50 min).

Discussion

Overview. In this work, we have rigorously established the phase diagram of a ternary MBS/MIL/Ch system at fixed buffered H_2O content that is crucial for understanding the physical state of aqueous-dispersed mixed dietary and biliary lipids in the lumen of the upper small intestine of adult human beings. We will describe first what is known concerning the phase behavior of the unitary and binary systems of the three lipid components in water. We will then compare and contrast the ternary digestive lipid system with dilute model biliary lipid systems, pointing out similarities and differences. Finally, we will discuss the fine structure and characteristics of the pathophysiologically relevant two-phase region of the present phase diagram (B_2 zone, Figure 2). In this connection, it is worth noting that, in model bile systems, the physiologically important boundary of the micellar phase is the upper one, i.e., toward the Ch apex of the triangle (Carey & Small, 1978), whereas in the model digestive lipid systems, it is the right-hand boundary, i.e., toward the swelling amphiphile apex of the triangle (Figure 2).

Binary Aqueous Lipid Systems. In aqueous electrolyte solutions, the common bile salts, whether single or mixed, exhibit cmc values <7.5 mM, have large micellar phases, and display no liquid-crystalline phenomena (Small, 1971; Carey, 1985). Over the entire pH range studied here (5.5–7.5), the pure MBS system was a single-phase micellar system (cmc = 1.34 mM) that was optically clear and, by QLS, was isotropic with micellar $\bar{R}_h$ values of 18–20 Å. Although, at pH 5.5, 10% of the glycine conjugates were undissociated (Figure 5), this concentration of otherwise insoluble bile acids was solubilized in micellar solution by the ionized glycine- and taurine-conjugated MBS without a phase separation occurring (Small, 1971). A simple calculation shows that, since total lipid concentration was held constant (Figure 2), the MBS concentration only approached a monomeric value (2.1 mM at 37 °C, a value *greater* than its cmc) when the one-phase liquid-crystalline zone (A_2) was entered. Because of the profound dependence of pK'_a values on BS concentrations exceeding their cmc values (Small, 1971; Igimi & Carey, 1980), pK'_a values of monomeric MBS would be less than MBS in the micellar phase by $\sim$1–2 pH units. Hence, within the two-phase physiological zone (B_2), the percent ionization of MBS is likely >95% at all pH values studied here.

The small amounts of MG, PL, and DG in the aqueous MIL system are effectively nonionic between pH 11 and 3 and, because of their low concentrations (Table II), should not appreciably alter the properties of various phases formed by the NaFA systems upon titration from very alkaline to very acid (Shankland, 1970). Further, it has been demonstrated that the phase transformations of aqueous FA as functions of pH (Cistola et al., 1988) are shifted to lower pH values by the presence of BS (compare Figure 5B with Figure 6A,B) and added ionic strength (Shankland, 1970). The pH-dependent FA aqueous systems are extremely complex (Shankland, 1970; Small, 1986) and may take days to attain true equilibrium (Cistola et al., 1988), as was verified at 23 °C in the present work. With pure long-chain FA/H_2O systems above the cmc values of the ionized species and well above the FA melting temperature (40 °C) (Cistola et al., 1988), there are pH-dependent continua from a one-phase micellar system at pH >9.5, a lamellar acid soap phase coexisting with saturated micelles (two-phase system) at pH $\sim$9.0, and only a lamellar phase with solubilized soap (A^-) between pH 9.0 and 7.7. When the pH was further lowered, final pH $\sim$7.0, a phase transition to FA oil occurred as excess undissociated FA precipitated from the acid soap. Cistola and colleagues (Cistola et al., 1988) have reported that, between pH 7.2 and pH 7.8, an unidentified phase, which could be an inverted cubic or other liquid-crystalline phase, is present in these systems. It is clear from our titration studies of mixtures plotting within the ternary system's micellar phase (A_1 zone, Figure 5B) and in the B_2 two-phase zone (Figure 6A) that, at pH 6.5 (arrows), the predominant physical state of FA was that of the 1:1 acid soap. This was further verified by the observation that, at pH 5.5 and 6.5 and when the MIL system contained a ratio of FA:MG of 10:1 and 20:1, an unidentified oil phase appeared only in the liquid-crystalline region (A_2), but never in the micellar (A_1) or physiological two-phase zone (B_2), of the phase diagram (Figure 2).

Temperature-dependent phase equilibria of Ch/H_2O systems are well-defined (Small, 1968). The aqueous solubility of Ch is $\sim 10^{-8}$ M at 30 °C (Saad & Higuchi, 1965). At higher concentrations, Ch/H_2O systems form two phases, Ch monohydrate crystals in equilibrium with Ch monomers in water. No micellar or liquid-crystalline phases occur in these systems.

The axes of the ternary system (Figure 2) describe the phase equilibria of the binary lipid mixtures in aqueous buffer (MBS/Ch/H_2O, Ch/MIL/H_2O, and MBS/MIL/H_2O). In

a 1 g/dL concentration, MBS and Ch (left axis, Figure 2) formed a small mixed micellar phase with a maximum Ch-solubilizing capacity of 1–1.5 mol %. As shown in Figures 3 and 4, 1–1.5 mol % micellar Ch had no appreciable influence on micellar size, a phenomenon noted previously for individual BS/Ch systems (Mazer et al., 1979; Carey et al., 1981). With higher Ch contents, two-phase zone B_1 was entered where mixed micelles saturated with Ch and Ch monohydrate crystals coexisted. This was quite analogous to the binary BS/Ch axis in the dilute model bile system of single BS/Ch/H_2O (Carey & Small, 1978).

In the 1 g/dL Ch/MIL system (right axis, Figure 2), pure MIL solubilized large amounts of Ch at pH 6.5 and 7.5 with saturation occurring at approximately equimolar Ch:MIL ratios. An identical saturation ratio has been observed for Ch/PL systems (Small, 1971) and is probably related to the observation that MIL at these pH values and PL (at all pH values from 2 to 12) form lamellar liquid crystals in water. Between the equimolar points on the right axis of Figure 2 and the Ch apex of the triangle, a two-phase region was entered where Ch crystals separated from the saturated Ch/MIL lamellar liquid crystals. However, with FA:MG ratios of 10:1 and 20:1 at pH 6.5 and pH 5.5, an additional oil phase was present in the pure MIL system and in zone A_2; the capacities of these two-phase MIL (±MBS) systems to solubilize Ch were not determined.

In the MBS/MIL system (base axis, Figure 2), the mixtures were micellar between 100% and ~58% MBS (Figures 2 and 3). As anticipated, the right boundary of the micellar phase varied markedly with total lipid concentration, pH, and FA:MG ratios (Figure 8). As the MIL:MBS molar ratio was increased (Figure 3), the micellar $\bar{R}_h$ values showed no alteration at first, and then only a gradual and slight increase in sizes as the micellar phase limit was approached. The QLS results (given in Figure 3) were consistent with the coexistence of 32-Å ($\bar{R}_h$) mixed micelles in equilibrium with variable proportions of 18-Å simple micelles (possibly containing a small amount of MIL) for *all* MIL:MBS ratios between 0.1 and 0.68. This was consistent with the fact that the imc for MBS/MIL micelles (3.5 mM) was appreciably greater than the cmc (1.34 mM, see Results) and thus would require the presence of excess simple micelles to raise the monomeric BS concentration to this level. It is noteworthy that Svärd and colleagues (Svärd et al., 1988) observed similar differences in cmc/imc estimates for the analogous sodium taurocholate/MG micellar systems. At the micellar phase limit, and as also occurred in the latter system (Svärd et al., 1988), there was an abrupt increase in particle sizes, heralding entrance into the two-phase zone, B_2 (Figure 2), where a coexistence of a vesicle phase in equilibrium with mixed micelles was found (Figures 7–9). This abrupt phase transition was clearly distinguishable from what was observed in BS/PL systems, where a gradual divergence in micellar sizes occurs at high PL:BS ratios but still within the micellar zone (Mazer et al., 1980), and formed the experimental basis for the "mixed disk" model of BS/PL micelles (Mazer et al., 1980). Indeed, the difference between imc and cmc in the MBS/MIL system may account for the lack of mixed micellar growth compared with BS/PL systems. In contrast to the MBS/MIL system, the imc values of taurocholate, taurodeoxycholate, glycocholate, and glycochenodeoxycholate in the presence of PL are appreciably *lower* than the cmc of the pure BS (Carey, 1985; Mazer et al., 1980; Schurtenberger et al., 1985). This is probably a reflection of the ability of BS to interact more favorably with BS/PL bilayers than with either simple micelles or BS/MIL bilayers and hence reflects the lack of strong mixed micellar growth in the latter (Figure 3).

Since the pK'_a of FA in BS micelles lies in the range pH 6.4–7.0 (Figure 5B) (Shankland, 1970; Hofmann, 1968), the solubilized MIL most likely existed as lamellar acid soap, i.e., NaH $(A^-)_2$, with the liquid FA chains of MG, PL, and traces of DG intermixed with the acyl groups of the acid soap. It is significant that the 1–3 mol % DG did not trigger a lamellar-to-inverted hexagonal phase transition as it does in PL systems (Siegel et al., 1989). It should be appreciated, however, that at pH 7.5 excess soap (A^-) molecules can be solubilized in the acid soap structure, but at pH 5.5 excess FA was probably phase-separated from the acid soap (Small, 1986; Cistola et al., 1988). Between ~59% and 20% MBS (base axes, Figure 2) and as shown under Results, there exists a two-phase system composed of spontaneously formed unilamellar vesicles and saturated mixed micelles (Figures 7 and 10). In a related system, sodium taurocholate/MG/water, Lindman and his colleagues (Schurtenberger et al., 1986; Svärd et al., 1988) also found weak micellar growth ($\bar{R}_h$ = 10–30 Å) even at compositions (by dilution) that plotted very close to the micellar phase limit and noted a transition to a coexistence of unilamellar vesicles and mixed micelles beyond the phase limit. The one-phase liquid-crystalline (A_2) phase was not studied systematically in our work, but contained, by QLS, particles with $\bar{R}_h$ values ≫5000 Å and macroscopic FA oils under conditions of low pH and high FA:MG ratios. While the molecular structures of these phases were not investigated, it is of interest that 1 g/dL pure 5:1 molar FA:MG systems (no BS) at pH 6.5 have been described as forming an L-2 (inverted micellar) phase (Lindström et al., 1981).

Ternary Lipid Systems: Micellar Phase A_1. The micellar phase was somewhat larger than sodium taurocholate/PL/Ch systems for the same total lipid concentration (Carey & Small, 1978). Provided that the evidence marshalled for the analogous behavior of MIL and PL in determining the extent of the micellar phase is reasonable, this difference suggests that the lower imc of the more hydrophobic BS in the MBS system was responsible (cmc/imc of taurocholate are 5–7.5 mM/3–5 mM) (Carey et al., 1981; Mazer et al., 1979; Mazer et al., 1980). The higher imc of NaTC/PL/mixed micellar systems resulted in more striking changes in the size of the micellar zone with dilution (Carey & Small, 1978). The degree of expansion of the micellar phase (MBS/MIL > taurocholate/PL) in the present work was therefore likely to be induced by the smaller magnitude of the imc (MBS) value (~3.5 mM), compared with that of the taurocholate/PL (Duane, 1977) and taurocholate/MG (Svärd et al., 1988) systems. For the same reasons, the maximum mole percent Ch solubilized in the micellar phase in the present work was greater than that observed for model bile systems of taurocholate/PL of the same concentration (1 g/dL) (Carey & Small, 1978). In this regard, it is notable that the present micellar Ch solubility of 5 g/dL systems (at pH 6.5) was similar to that obtained by Montet and colleagues (Montet et al., 1979) for 4 g/dL sodium taurochenodeoxycholate and sodium taurocholate/FA/MG (2:1) at pH 6.7 (37 °C). Recently, these investigators (Reynier et al., 1987) delineated Ch solubilities in the micellar phase of sodium taurocholate/FA:MG (2:1 molar ratio) with total lipid concentrations that varied continuously but that approached ~1 g/dL at the right-hand micellar phase boundary. In the former work, the authors (Montet et al., 1979) found maximum Ch solubility at ~50% NaTCDC plus NaTC and observed that the micellar phase boundary intersected the base line at 40% BS, i.e., an

expansion of the micellar phase to the right, which disagrees with the present work. In their later work (Reynier et al., 1987), maximum Ch solubility (4 mol %) fell at 64% sodium taurocholate, and the micellar phase boundary intersected the base line at 48.5% BS. In an earlier approach to this problem, we (Stafford & Carey, 1981; Stafford et al., 1981; Carey et al., 1983) reported (in abstract form) that the micellar phase limit for 1 and 2 g/dL systems was at 45% BS, that a maximum of 8% Ch could be solubilized, and that micellar $\bar{R}_h$ values were as large as 100–200 Å. These results disagree with the present work, and the implications are important, since errors in determination of the micellar phase limit would not only place many physiological lipid compositions incorrectly within the micellar zone [see Hernell et al. (1990)] but give apparent values for "micellar" sizes that were, in fact, due to vesicles. We therefore believe that determinations of micellar phase boundaries in such multicomponent lipid systems at very high dilution (simulating physiological conditions), utilizing only polarizing microscopy and visible Tyndall phenomena as employed by us earlier (Carey et al., 1983) and by Montet and colleagues (Montet et al., 1979; Raynier et al., 1987), are very imprecise. As indicated under Results, we found that unaided optical observations correlated very poorly with QLS determinations of micellar phase boundaries and generally resulted in overestimates. The principal reason is apparent from Figures 7 and 9, where many of the vesicle sizes in the two-phase (B_2) zone were considerably less than 1000 Å in diameter and therefore would scatter insufficient light for detection by the unaided eye. Further, unilamellar vesicles in the B_2 zone of Figure 2 are not birefringent and are too small to be detected by either direct or polarized light microscopy.

Expansion of the micellar phase by increases in total lipids and pH and by a 2- and 4-fold increase in FA:MG ratio (Figure 8) may have related explanations. It is likely that the micellar phase expands with the greater content of partially ionized FA as acid soap. As inferred from physical–chemical studies of long-chain FA without BS as functions of pH, this was clearly aided by increased ionization (Cistola et al., 1988). Second, increasing the FA:MG ratio at pH 6.5 decreases the concentration of spacer molecules of MG to be solubilized, and hence, as shown here, there was a higher capacity to solubilize the acid soap lamellae as mixed micelles. These findings are in disagreement with the work of Hofmann (1968), who noted that FA acid soaps and MG have, on a molar basis, similar solubilities in BS micelles.

The Physiologically Important Two-Phase Zone (B_2). Within the limits of the present methods, the B_2 zone contained only two phases (mixed micelles and unilamellar vesicles) dispersed in the aqueous buffer under all physical–chemical conditions at equilibrium. This was best demonstrated by the tie-lines in Figure 10, where MBS mixed micelles saturated with MIL and Ch and unilamellar vesicles saturated with MBS but, apparently, *not* with Ch, were ultracentrifugally separated. Within experimental error of lipid quantitation by thin-layer chromatography and densitometry (±10%; see Methods), the relative lipid composition of the separated phases plotted on the micellar and liquid-crystalline phase boundaries, respectively. Because of the data dispersion in Figure 10, we cannot exclude the possibilities that thin bands of dispersed hexagonal (rod) (Carey, 1988) or cubic phases (Mariani et al., 1988) may coexist under certain physical–chemical conditions in the B_2 zone of these systems, as we suggested earlier (Patton & Carey, 1979). Indeed, in the analogous taurocholate/MG/water phase diagram, Svärd and co-workers (Svärd et al., 1988) obtained NMR and polarizing microscopic evidence for the presence of presumed hexagonal and "ribbon"-like phases occurring between the isotropic micellar and lamellar liquid-crystalline phases, but it proved impossible for these authors to obtain one-phase samples for unequivocal X-ray analysis.

As is well-known from other systems (Mazer et al., 1980; Mazer & Carey, 1983), mixed micelles equilibrated very rapidly following the addition of aqueous buffer to lipid coprecipitates in the present work (Figure 1); this likely occurred in the case of coexisting micelles in the two-phase (B_2) zone also (Figures 1 and 2). However, the vesicle phase in this zone took 3–5 days to reach equilibrium sizes at 37 °C (Figure 1). Further, 3–8 mol % Ch was incorporated into vesicles of intermediate size with no appreciable influence on their sizes or equilibria (see Figures 3 and 4), as noted by other authors (Szoka & Papahadjopoulos, 1980). Nonetheless, the dynamics of vesicles that coexisted with micelles were very different from those of pure vesicle systems. For example, with lipid ratios in the two-phase (B_2) zone that plotted close to the micellar phase boundary (Figure 1) vesicle sizes grew with passage of time. This was most likely related to the rapid formation of MIL-supersaturated mixed MBS micelles upon the addition of aqueous buffer that then "spawned" a population of MIL/MBS vesicles as the systems equilibrated [see Cohen (1986) and Cohen et al. (1989)]. With lipid ratios well within the B_2 zone, i.e., with higher MIL compositions (Figure 1), the decrease in vesicle sizes was most likely induced by BS-mediated lipid exchange between a population of larger and smaller vesicles (Nichols, 1986). In fact, as shown elsewhere (Cohen, 1986; Cohen et al., 1989), perimicellar concentrations of BS, as is the case for these mixtures (see imc values under Results), rapidly homogenize vesicles of different sizes into a unimodal population. This was verified in part by the scattered light intensity from vesicles (Figure 11, panels C and D), which indicated that smaller vesicles coexisted with larger vesicles for compositions that plotted close to the micellar phase limit, as well as by the heterogeneity in vesicle sizes (<-150–>600-Å radius) in the freeze-fracture electron micrographs (Figure 7).

Finally, because of their putative physiological importance in vivo, it was important to demonstrate that vesicles in the B_2 zone (Figure 2) underwent rapid spontaneous dissolution into unsaturated mixed micellar solutions of the A_1 zone (Table III and Figure 12). Dissolution rates were critically dependent upon both the MIL and Ch saturations of the micellar solutions. These results strongly suggest that, during TG digestion in the upper small intestine of adult human beings [see Hernell et al. (1990)], the coexistence of vesicles with mixed micelles will be dependent upon a balance between the rates of their production and those of their dissolution, with the latter depending critically upon the degree of unsaturation of coexisting BS mixed micelles. If micellar saturation with MIL proves physiologically to be a common phenomenon (Carey et al., 1983), especially if the production of lipolytic products is much faster than micellar dissolution to saturation and subsequent mucosal absorption, then vesicles will be a metastable, dispersed physical state of swelling amphiphilic lipids that will be of physiologic importance in human fat digestion and absorption. The framework of these results is employed in an investigation of the physical state of dietary and biliary lipids during human fat digestion and absorption addressed in the accompanying paper (Hernell et al., 1990).

ACKNOWLEDGMENTS

We thank Dr. David E. Cohen for his expert advice and assistance with QLS analysis, Dr. James Madara for freeze-

fracture electron microscopy, Heideh K. Ahari for technical help, and Rebecca Ankener for superb word-processing, editorial, and bibliographic assistance. We are particularly indebted to Professor Bengt Borgström and an anonymous reviewer for their thorough and constructive criticisms of the manuscript.

Registry No. Ch, 5808-12-8; FA, 112-80-1; MG, 30836-40-9; sodium hydrogen dioleate, 124225-51-0.

References

Back, E., & Steenberg, B. (1950) *Acta Chem. Scand. 4*, 810–815.

Bartlett, G. R. (1959) *J. Biol. Chem. 234*, 466–468.

Bitman, J., & Wood, D. L. (1981) *J. Liq. Chromatogr. 4*, 1023–1034.

Bitman, J., Wood, D. L., & Ruth, J. M. (1981) *J. Liq. Chromatogr. 4*, 1007–1021.

Borgström, B. (1977) *Int. Rev. Physiol. 12*, 305–323.

Borgström, B. (1985) *Scand. J. Gastroenterol. 20*, 389–394.

Carey, M. C. (1983) in *Bile Acids in Gastroenterology* (Barbara, L., Dowling, R. H., Hofmann, A. F., & Roda, E., Eds.) pp 19–56, MTP Press, Boston.

Carey, M. C. (1985) in *Sterols and Bile Acids* (Danielsson, H., & Sjövall, J., Eds.) pp 345–403, Elsevier, Amsterdam.

Carey, M. C. (1988) in *Bile Acids in Health and Disease* (Northfield, T., Jazrawi, R., & Zentler-Munro, P., Eds.) pp 61–82, Kluwer, Lancaster, U.K.

Carey, M. C., & Small, D. M. (1969) *J. Colloid Interface Sci. 31*, 383–396.

Carey, M. C., & Small, D. M. (1978) *J. Clin. Invest. 61*, 998–1026.

Carey, M. C., Montet, J. C., Phillips, M. C., Armstrong, M. J., & Mazer, N. A. (1981) *Biochemistry 20*, 3637–3648.

Carey, M. C., Small, D. M., & Bliss, C. M. (1983) *Annu. Rev. Physiol. 45*, 651–677.

Cistola, D. P., Hamilton, J. A., Jackson, D., & Small, D. M. (1988) *Biochemistry 27*, 1881–1888.

Cohen, D. E. (1986) Ph.D. Dissertation, Harvard University, 8806072, pp 1–207, University Microfilms, Ann Arbor, MI, 1988.

Cohen, D. E., Angelico, M., & Carey, M. C. (1989) *Am. J. Physiol. 20*, G1–G8.

Cohen, D. E., Fisch, M. R., & Carey, M. C. (1990) *Hepatology* (in press).

Duane, W. C. (1977) *Biochem. Biophys. Res. Commun. 74*, 223–229.

Folch, J., Lees, M., & Sloane-Stanley, G. H. (1957) *J. Biol. Chem. 226*, 497–509.

Hernell, O., Staggers, J. E., & Carey, M. C. (1990) *Biochemistry* (following paper in this issue).

Hofmann, A. F. (1968) *Adv. Chem. Ser. 84*, 53–66.

Hofmann, A. F. (1976) *Adv. Intern. Med. 21*, 501–534.

Hofmann, A. F., & Borgström, B. (1962) *Fed. Proc. 21*, 43–50.

Hofmann, A. F., & Borgström, B. (1964) *J. Clin. Invest. 43*, 247–257.

Igimi, H., & Carey, M. C. (1980) *J. Lipid Res. 21*, 72–90.

Larsson, K. (1967) *Z. Phys. Chem. 56*, 173–198.

Lindström, M., Ljusberg-Wahren, H., Larsson, K., & Borgström, B. (1981) *Lipids 16*, 749–754.

Madara, J. L. (1983) *J. Cell Biol. 97*, 125–136.

Mansbach, C. M., Cohen, R. S., & Leff, P. B. (1975) *J. Clin. Invest. 56*, 781–791.

Mariani, P., Luzzati, V., & Delacroix, H. (1988) *J. Mol. Biol. 204*, 165–189.

Mazer, N. A., & Carey, M. C. (1983) *Biochemistry 22*, 426–442.

Mazer, N. A., Benedek, G. B., & Carey, M. C. (1976) *J. Phys. Chem. 80*, 1075–1085.

Mazer, N. A., Carey, M. C., Kwasnick, R. F., & Benedek, G. B. (1979) *Biochemistry 18*, 3064–3075.

Mazer, N. A., Benedek, G. B., & Carey, M. C. (1980) *Biochemistry 19*, 601–615.

Miettinen, T. A., & Siurala, M. (1971) *Scand. J. Gastroenterol. 6*, 527–535.

Montet, J. C., Reynier, M. O., Montet, A. M., & Gerolami, A. (1979) *Biochim. Biophys. Acta 575*, 289–294.

Nichols, J. W. (1986) *Biochemistry 25*, 4596–4601.

Patton, J. S. (1981) in *Physiology of the Gastrointestinal Tract* (Johnson, L. R., Ed.) pp 1123–1146, Raven Press, New York.

Patton, J. S., & Carey, M. C. (1979) *Science 204*, 145–148.

Porter, H. P., & Saunders, D. R. (1971) *Gastroenterology 60*, 997–1007.

Reynier, M. O., Crotte, C., Montet, J.-C., Sauve, P., & Gerolami, A. (1987) *Lipids 22*, 28–32.

Ricour, C., & Rey, J. (1970) *Rev. Eur. Etud. Clin. Biol. 15*, 287–293.

Saad, H. Y., & Higuchi, W. I. (1965). *J. Pharm. Sci. 54*, 1205–1206.

Schurtenberger, P., Mazer, N., & Känzig, W. (1985) *J. Phys. Chem. 89*, 1042–1049.

Schurtenberger, P., Svärd, M., Wehrli, E., & Lindman, B. (1986) *Biochim. Biophys. Acta 882*, 465–468.

Shankland, W. (1970) *J. Colloid Interface Sci. 34*, 9–25.

Siegel, D. P., Banschbach, J., & Yeagle, P. L. (1989) *Biochemistry 28*, 5010–5019.

Small, D. M. (1968) *J. Am. Oil Chemists Soc. 45*, 108–119.

Small, D. M. (1971) in *The Bile Acids* (Nair, P. P., & Kritchevsky, D., Eds.) pp 249–356, Plenum Press, New York.

Small, D. M. (1986) *The Physical Chemistry of Lipids*, pp 285–343, Plenum Press, New York.

Stafford, R. J., & Carey, M. C. (1981) *Clin. Res. 29*, 511A.

Stafford, R. J., Donovan, J. M., Benedek, G. B., & Carey, M. C. (1981) *Gastroenterology 80*, 1291 (Abstract).

Staggers, J. E., Frost, S. C., & Wells, M. A. (1982) *J. Lipid Res. 23*, 1143–1150.

Staggers, J. E., Hernell, O., & Carey, M. C. (1986) *Biophys. J. 49*, 325A.

Svärd, M., Schurtenberger, P., Fontell, K., Jönsson, B., & Lindman, B. (1988) *J. Phys. Chem. 92*, 2261–2270.

Szoka, F., Jr., & Papahadjopoulos, D. (1980) *Annu. Rev. Biophys. Bioeng. 9*, 467–508.

Thompson, G. R., Barrowman, J., Gutierrez, L., & Dowling, R. H. (1971) *J. Clin. Invest. 50*, 318–323.

Turley, S. D., & Dietschy, J. M. (1978) *J. Lipid Res. 19*, 924–928.